

Combining Optical and Raman Spectroscopy with Electrochemistry: The Ferricyanide and Ferrocyanide System - Experiments for Undergraduates

A. Habekost*

University of Education Ludwigsburg, Ludwigsburg, Germany

*Corresponding author: A.Habekost@t-online.de

Received February 06, 2024; Revised March 09, 2024; Accepted March 15, 2024

Abstract Ferricyanide and ferrocyanide are often used in undergraduate education to experimentally investigate the redox behaviour, the different thermodynamic stability and the formation of Prussian Blue. Surface-enhanced Raman scattering (SERS) on colloids is intensively studied in chemistry, but the didactic implications in terms of developing easy-to-perform experiments have not been intensively discussed. These experiments show the spectroelectrochemical behaviour (optical and Raman) of the redox system on gold and silver electrodes at different potentials. The SERS experiments show that the Raman modes are changed due to the strong adsorption on the electrochemically prepared Au and Ag surfaces. Prussian blue can be easily prepared electrochemically.

Keywords: (Surface enhanced) Raman Spectroscopy, absorptovoltammetry

Cite This Article: A. Habekost, "Combining Optical and Raman Spectroscopy with Electrochemistry: The Ferricyanide and Ferrocyanide System - Experiments for Undergraduates." World Journal of Chemical Education, vol. 12, no. 1 (2024): 30-38. doi: 10.12691/wjce-12-1-5.

1. Introduction

Ten years after the use of Raman spectroscopy to study the adsorption of pyridine on silver electrodes by Fleischmann et al [1,2], the ferricyanide/ferrocyanide system was studied by the same author using surface enhanced Raman spectroscopy (SERS) on different electrodes [3]. They show that the frequencies of the Fe-C and C-N stretching modes (A_{1g} and E_g , see Figure 1) vary with the cation used and the applied potential.

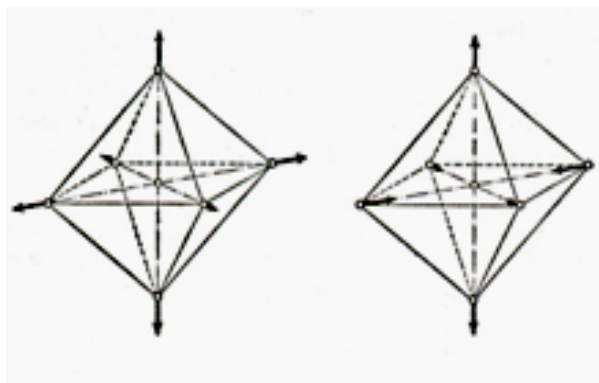


Figure 1. A_{1g} (left) and E_g (right) modes [4]

For K^+ the authors found the following cyanide frequencies for ferrocyanide ($K_3[Fe(CN)_6]$) as a function of the potential applied to an Au electrode:

Table 1. Potential dependent C-N stretching frequencies [3]

Potential / V	Frequency / $1/cm$
+0.4	2150
+0.3	2150
+0.2	2150
0	2125 and 2093
-0.2	2127

The following C-N frequencies of the ferrocyanide and the ferricyanide are measured in the solid state and in aqueous solution:

Fleischmann et al. found that the Raman modes differ as a function of the cations used. They conclude that the cations must be co-adsorbed on the surface. In contrast to the Raman spectra in solution, the SERS spectra on Au are shifted to higher frequencies. The authors explain this with the π^* orbital of the nitril group, which is involved in binding to the electrode. Another possible interpretation is that the lone pair of the nitrogen interacts with the electrode surface.

Spectroelectrochemistry is the combination of spectral (Raman and optical) information during changes in electrochemical behaviour [7]: In the case of ferri/ferrocyanide, the optical and Raman features must change during single electron transfer, see the cyclic voltammogram in Figure 2. The anodic peak at 0.26 V indicates oxidation ferricyanide-ferrocyanide, the cathodic peak at 0.17 V the reverse reduction.

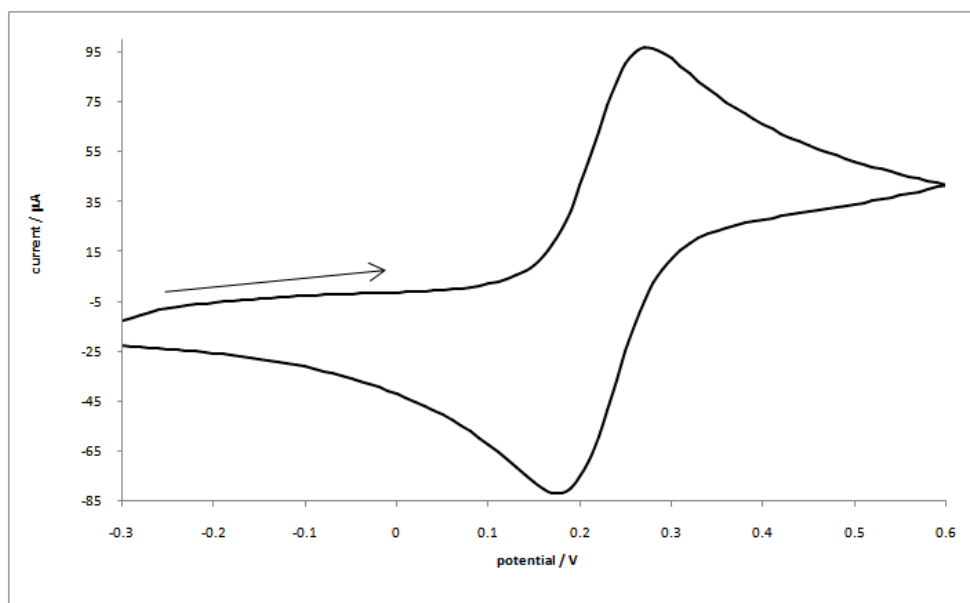


Figure 2. Cyclic voltammogram of ferricyanide on a Pt electrode. Arrow indicates the scan direction. Scan rate: 0.05 V/s

2. Experiments

2.1. Instruments and Chemicals

Materials: Potentiostat (μ Stat 400 from Metrohm / DropSens), Raman spectrometer (AvaRaman, Avantes, laser 785 nm, excitation fiber 200 μ m, 0.5 numerical aperture, collecting fiber 400 μ m), Raman cell (Metrohm / DropSens), fiber spectrometer (AvaSpec-ULS2048XL-EVO-RS-UA from Avantes), AvaLight-DH-S-BAL (deuterium and halogen lamp), SPE: DRP 220 Au-Bt (Metrohm / DropSens: working electrode: low-temperature gold ink, counter electrode: gold, pseudo reference electrode: silver), DRP 010 (Metrohm / DropSens: working electrode: silver, counter electrode: silver, pseudo reference electrode: silver) DRP-ITO (Metrohm / DropSens: working electrode: Indium-Tin oxide, counter electrode: carbon, pseudo reference electrode: silver), 420 nm LED (403101 from pur-led Technik (<https://www.pur-led.de/leuchtdioden/led-3mm-uv-420nm-schwarzlicht-ca-20mw-sr-abstrahlwinkel-ca-25.html>)).

Software: DropView (Metrohm / DropSens), Spectragryph (Version 1.2.16.1, Dr. Menges), Avasoft (Avantes), Qtiplot 0.9.9, IONDEF.

Chemicals: $K_4[Fe(CN)_6] \cdot 3H_2O$ and $K_3[Fe(CN)_6]$ (Carl Roth, Germany), Ammonium iron(III) sulphate $NH_4Fe^{III}(SO_4)_2 \cdot 12 H_2O$ (Merck, 3776), SERS Strips Ag (Metrohm, 607506160), Au-nanoparticles (DRP-AuNp-Col, Metrohm/DropSens).

Concentration of ferrocyanide and ferricyanide: 1 mmol in 10 mmol KCl.

Procedure: To create nanostructured Ag and Au surfaces, the SPE was coated with a 1 mmol solution of KCl. Three consecutive cyclic voltammograms were then recorded. Ag: -0.5 V to 0.5 V and vice versa. Au: -0.5 V to 1.5 V and vice versa: EC SERS.

2.2. Results

2.2.1. Raman Spectra (Solid and Aqueous Solution)

The Raman spectra for ferri/ferrocyanide show that the frequencies of the CN vibration correlate with those of Fleischmann (Figure 2) [3]. Due to the resolution of the Raman spectrometer used (4 cm^{-1}) there are only minimal differences of about $2\text{-}4 \text{ cm}^{-1}$. The two Raman frequencies of ferrocyanide (solid: 2136 and 2131 cm^{-1}) cannot be resolved with our instrument.

The Fe-C frequencies are of much lower intensity (Figure 3, Figure 4 left).

The spectra of ferricyanide can be discussed in two different regions: the low frequency region from $300\text{-}700 \text{ cm}^{-1}$ and the high frequency region from 1900 to 2200 cm^{-1} .

In the low frequency region the Fe-C stretching and bending modes can be found. The deviation from Loo [5] results from the different experimental conditions, see Table 2. The values are in good agreement with Griffith [6].

In the case of the ferricyanide solution, two Raman bands at $2100 (A_{1g})$ and $2065 \text{ cm}^{-1} (E_g)$ can be observed in the high frequency or nitrile stretching region.

2.2.2. EC-SERS Spectra

However, the electrochemically generated EC-SERS spectra show various differences depending on the Au and Ag surfaces used (Figure 5).

It is clear that the SERS spectrum on Au is shifted towards higher frequencies (around 40 cm^{-1} : red dashed line). The SERS spectrum on Ag is much broader, i.e. the peaks are less resolved (black dashed line). Compared to the solid phase of $K_4[Fe(CN)_6]$, both A_{1g} and E_g peaks are shifted downwards on Ag (A_{1g} : 2100 to 2092 cm^{-1} , E_g : 2069 to 2058 cm^{-1}). This is in agreement with Loo et al [5]. The shoulder at 2130 cm^{-1} , measured by Loo could not be observed on our SERS Ag surface.

Figure 6 shows that on commercially available nanostructures and in the presence of Au nanoparticles, the Raman peaks are broadened and partially shifted (the SERS spectra of $K_3[Fe(CN)_6]$ show the analogue behaviour).

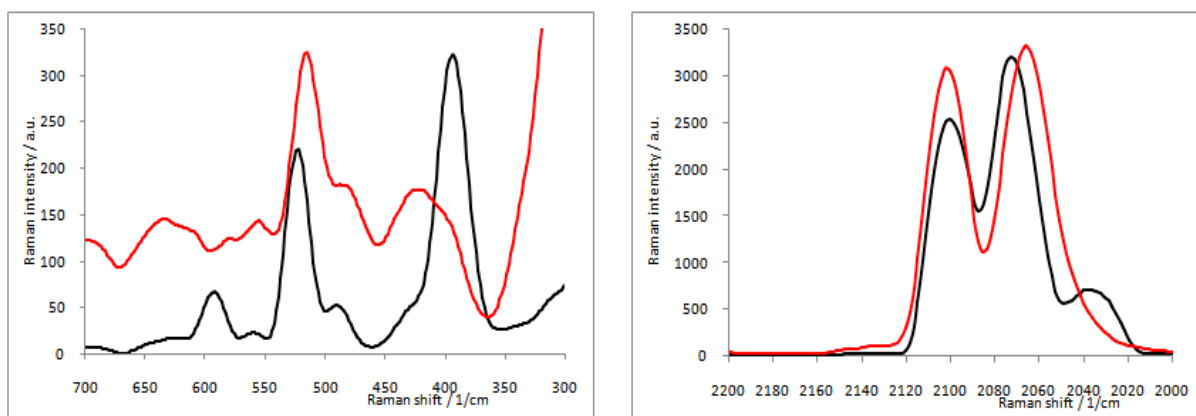


Figure 3. Raman spectra of $K_4[Fe(CN)_6]$. Black: solid, red: solution. Two different vibration regions

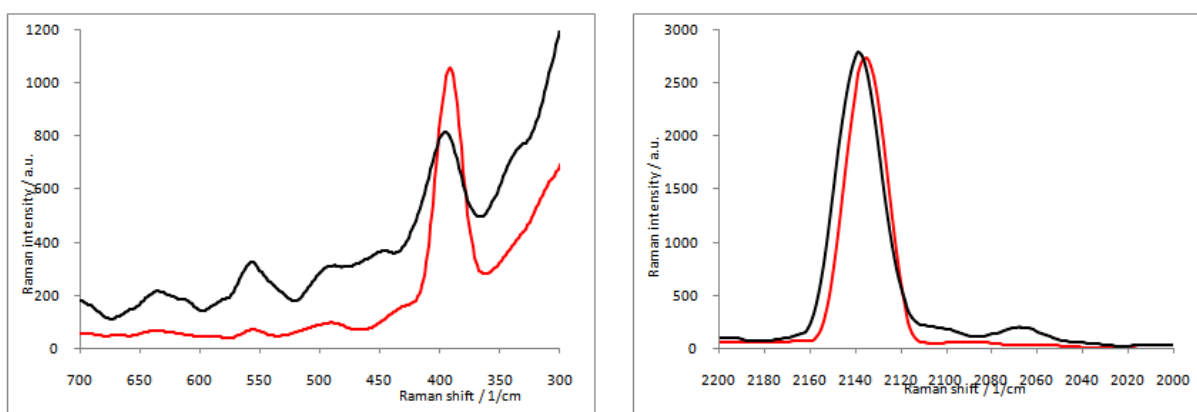


Figure 4. Raman spectra of $K_3[Fe(CN)_6]$. Black: solid, red: solution. Two different regions

Table 2. Wavenumbers from Fleischmann [3] in brackets from Loo [5] and cursive from Griffith [6]

Ferrocyanide solid / cm^{-1}	Ferrocyanide solution / cm^{-1}	Ferrocyanide solution / cm^{-1}	Ferricyanide solid / cm^{-1}	Ferricyanide solution / cm^{-1}	Ferricyanide solution (on an Ag-electrode at -1.00 V) / cm^{-1}
2136, 2135	2135, 2136 (A_{1g})	336, 392, 420	2094	2098 (2095) (A_{1g})	(560, 494) 396, 420 and 516.
2131	2129 2129, 2131 (E_g)		2063	2062 (2058) (E_g)	(423,373)

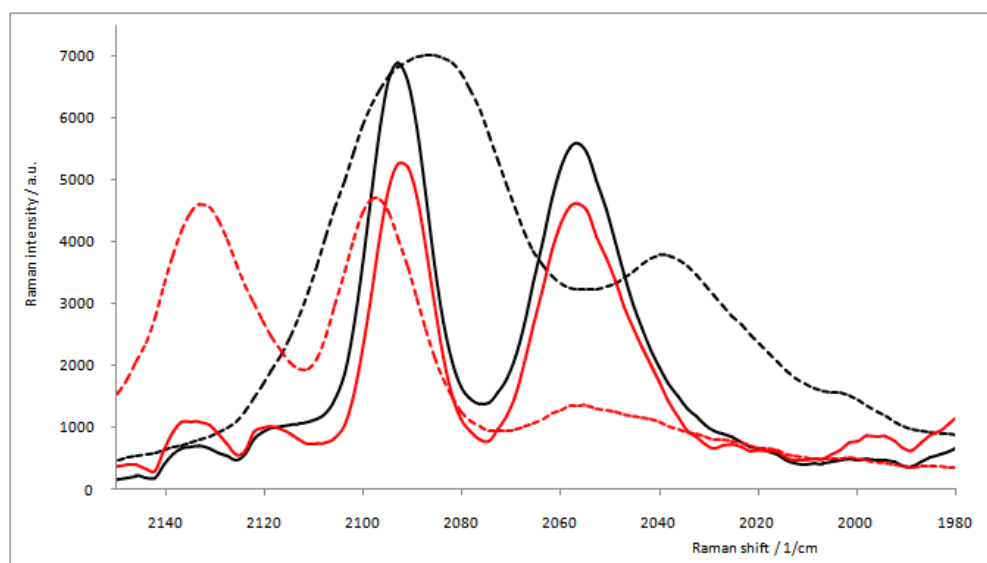


Figure 5. SERS spectra of $K_4[Fe(CN)_6]$ high frequency region on different surfaces. Black: Ag, red: Au. Dashed lines: SERS. Integration time metallic surfaces: 10s, on SERS colloid metals: 1s

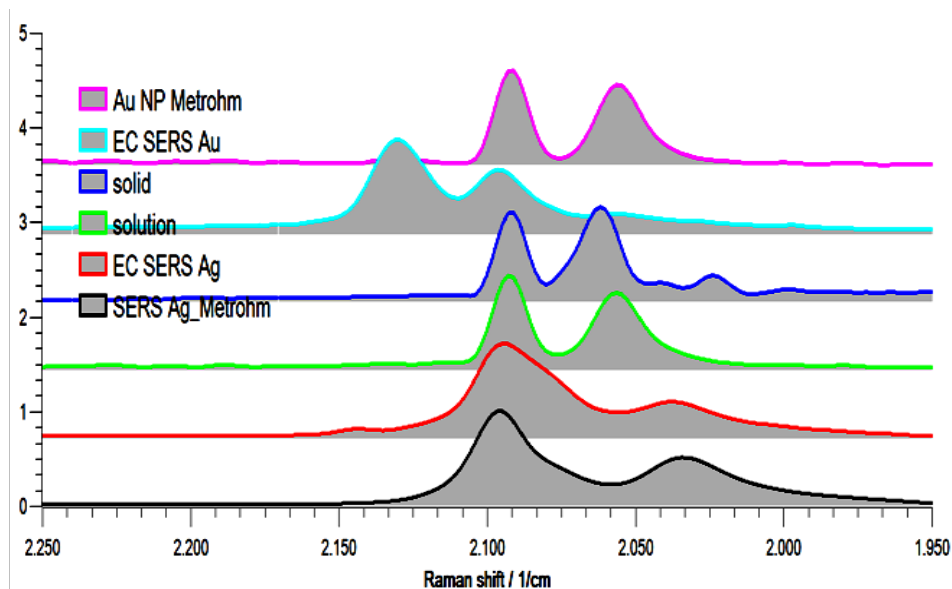


Figure 6. Comparison of SERS spectra of $K_4[Fe(CN)_6]$ high the frequency region on different, partly commercial, surfaces

2.2.3. Ramanvoltammograms

The discovery of the SERS effect from an electrochemical experiment (EC-SERS) is considered a historical breakthrough [8] because it opens up a method with a very low detection limit in analytical chemistry.

Figure 7 shows the SERS Raman spectra on Ag at different potentials, the low frequency region on the left and the high frequency region on the right. It is obvious that the Raman intensities increase at potentials from 0 V to -0.5 V, where the Ag nanoparticles are formed [9]. Between 0.5 V and -0.5 V the Raman frequency shifts by about 7 cm^{-1} towards higher frequencies.

Figure 8 shows the Ramanvoltammogram of the 2085 cm^{-1} vibration of $K_3[Fe(CN)_6]$.

$K_4[Fe(CN)_6]$ shows a similar behavior: From -0.3 V to 0.6 V the A_{1g} and E_g peaks increase in intensity and only the A_{1g} mode is shifted to lower frequencies (Figure 9).

2.2.4. Absorption spectra of ferrocyanine and ferricyanine

Figure 10 shows the absorption spectra of ferrocyanine (red) and ferricyanine (black). The spectra suggest that the main differences are in the region around 300 nm and 420 nm (see the difference spectrum in Figure 10).

Two different experimental setups were used to measure the absorptovoltammograms, as shown in Figure 11. The integral absorptovoltammogram was measured using a 420 nm LED for excitation and a photodiode for detection (Figure 11, left). A deuterium/halogen lamp combination was used for the spectrally resolved absorptovoltammogram. A fiber spectrometer was used as the detector (Figure 10, right). The main advantage of the former is its high sensitivity, while the latter has the additional spectral information during the electrochemical process.

Figure 12, top shows the potential dependent UV-VIS spectrum, Figure 12, bottom the absorption voltammogram between 350 and 450 nm for the oxidation and reduction of ferricyanide between -0.4 V and 0.6 V and vice versa.

The absorption of the formed ferricyanide increases up to about 0.2 V and decreases in the reverse run as the ferrocyanide is formed again.

Using a 420 nm LED (the absorption wavelength of ferrocyanide) the change in absorption is more pronounced, as shown in Figure 13.

The absorptovoltammogram in Figure 13 shows the excellent correlation between CV and derived absorbance.

Both EC-SERS and absorptovoltammetry are sensitive methods for correlating the electrochemical reaction with changes in Raman and optical properties.

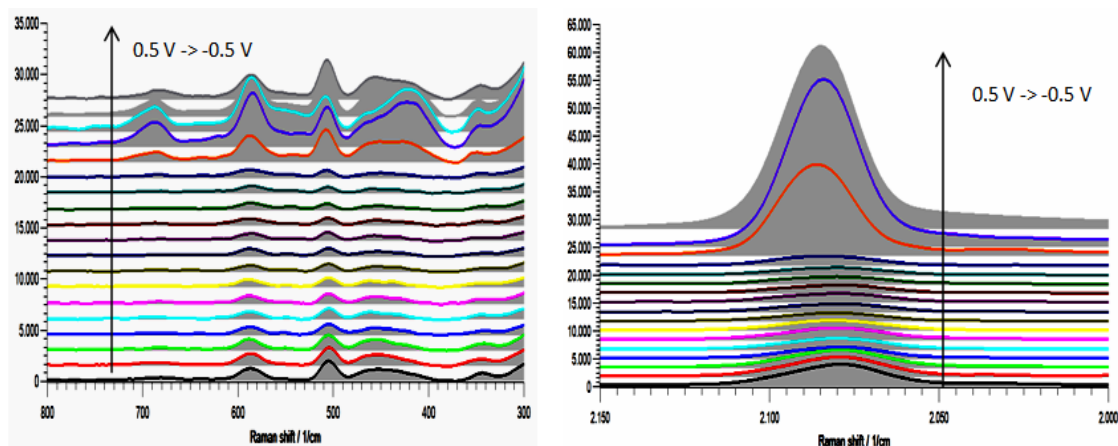


Figure 7. Potential dependent SERS Raman spectra of $K_3[Fe(CN)_6]$. Left: low frequency region, right: high frequency region

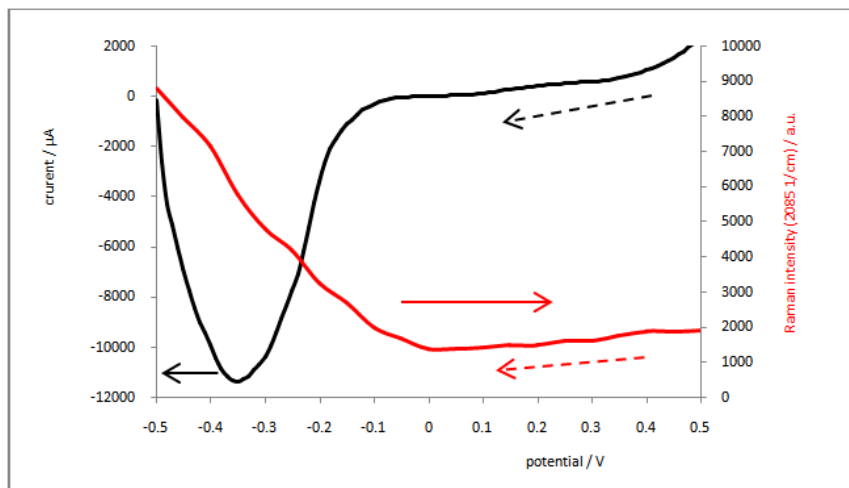


Figure 8. SERS-Ramanvoltammogram of the 2085 cm^{-1} Raman frequency of $\text{K}_3[\text{Fe}(\text{CN})_6]$ from $+0.5\text{ V}$ to -0.5 V on Ag. Dashed arrows: Scan direction

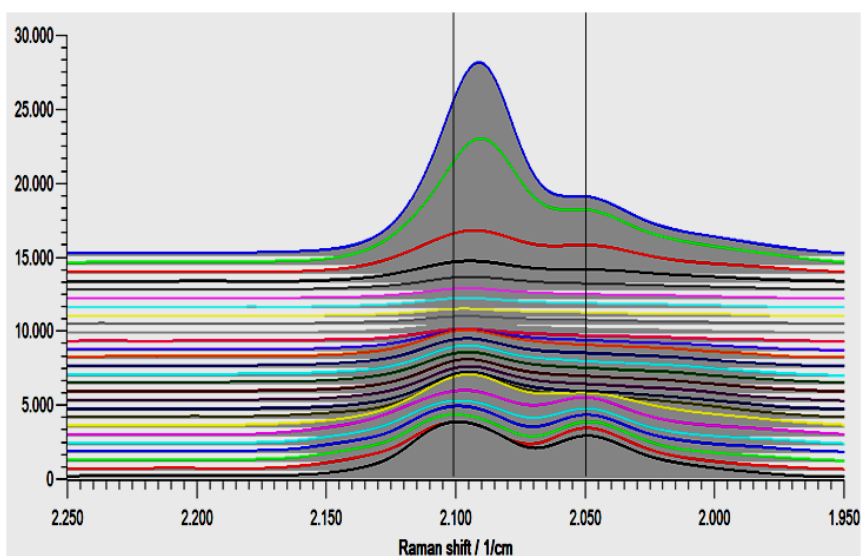


Figure 9. Potential dependent SERS Raman spectra of $\text{K}_4[\text{Fe}(\text{CN})_6]$. Potential from -0.3 V to $+0.6\text{ V}$. The A_{1g} frequency shifts from 2100 cm^{-1} (at -0.3 V) to about 2090 cm^{-1} (at 0.6 V)

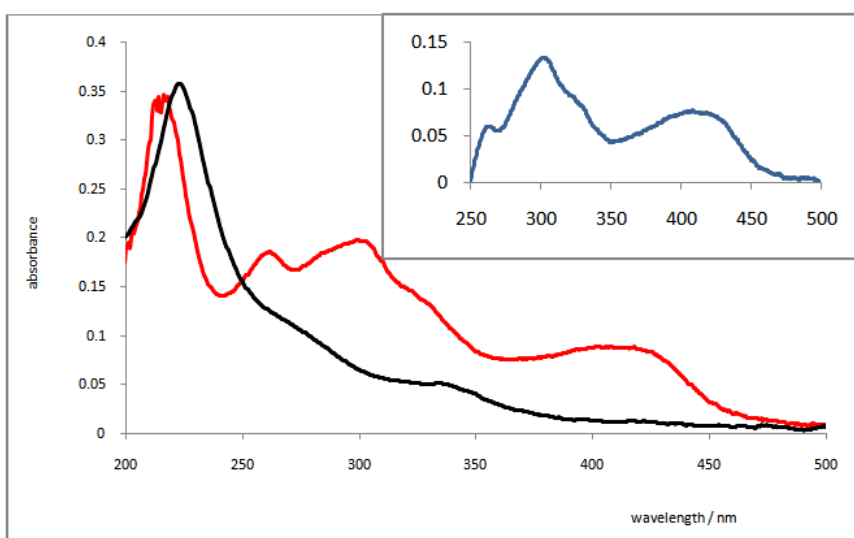


Figure 10. Absorption spectra of ferrocyanine (red) and ferricyanine (black). Inset: difference spectrum

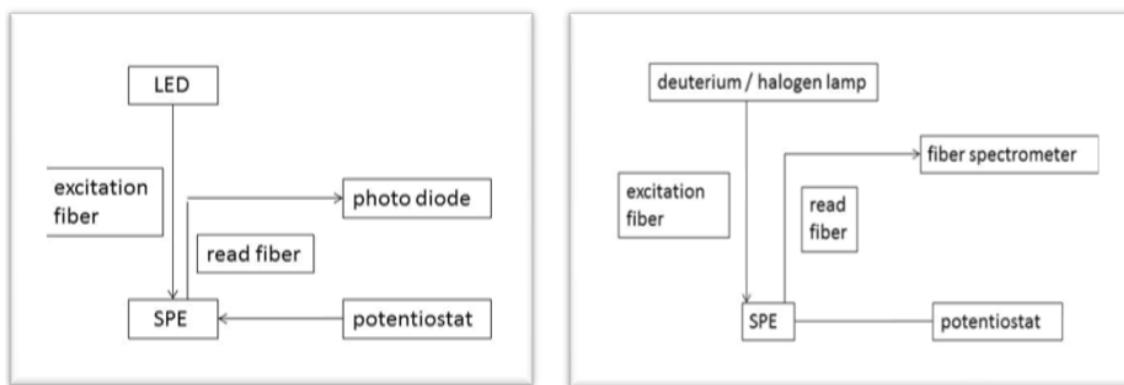


Figure 11. Left: Integral absorptovoltammogram, right: Spectral resolved absorptovoltammogram

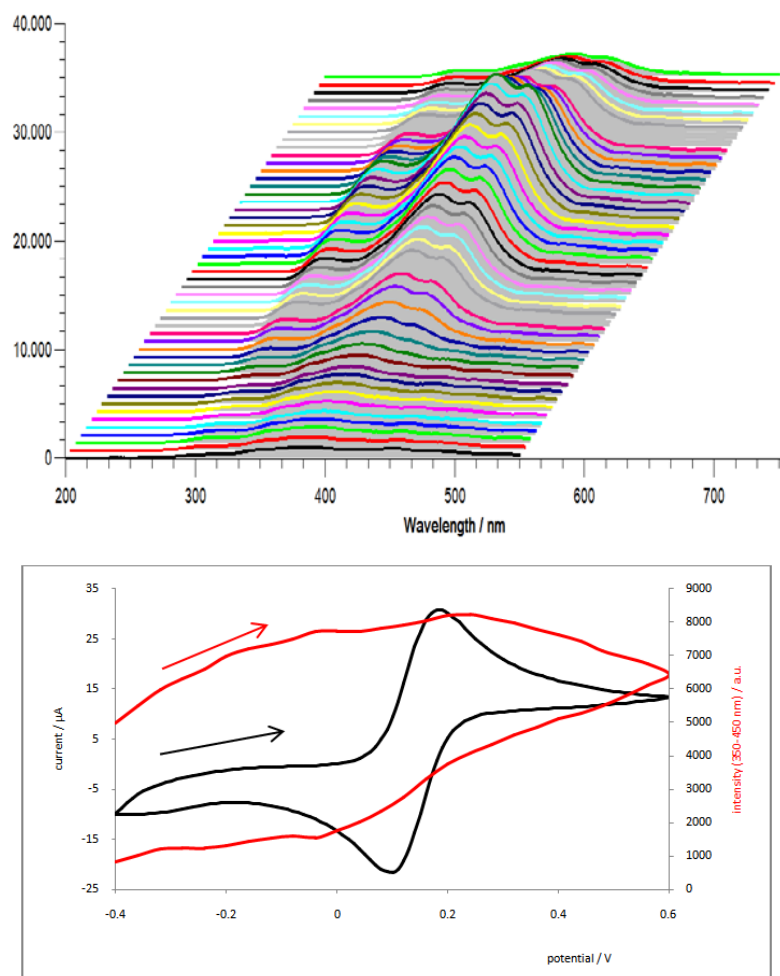
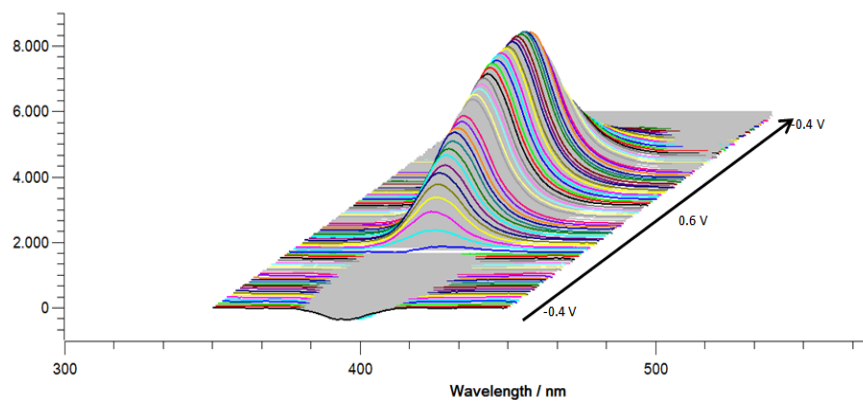


Figure 12. Top: Absorption spectra of ferricyanine between -0.4 and 0.6 V on a Pt electrode and vice versa. Bottom: Resulting Absorptovoltammogram at 350-450 nm



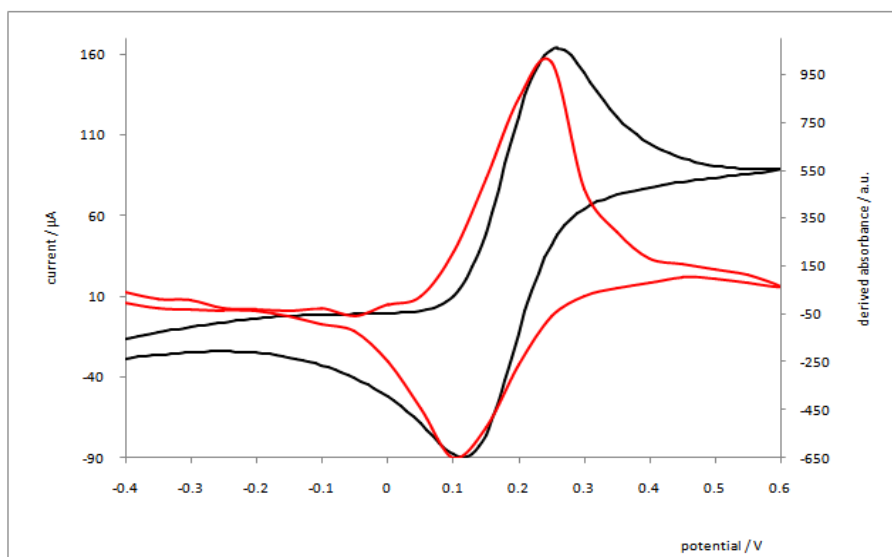


Figure 13. Top. Potential dependent absorption of ferri/ferrocyanide at 420 nm. Bottom: Derived Absorptovoltammogram (red line) and cyclic voltammogram (black line). Scan rate 50 mV/s, Pt SPE

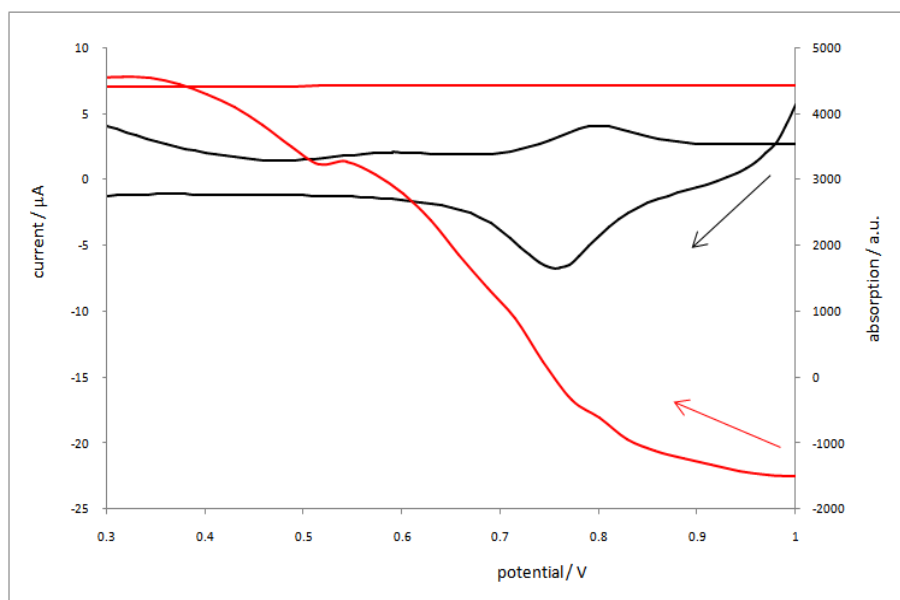


Figure 14. CV (black) and absorption (red) of a solution of $K_3[Fe(CN)_6]$ and Fe(III) salt. SPE: ITO

2.2.5. Electrochemically Produced Prussian Blue

Prussian blue can be easily prepared by applying an appropriate potential to an aqueous solution of $K_3[Fe(CN)_6]$ and Fe(III) [10,11]. By scanning the potential from 1 V to 0.3 V, starting at about 0.8 V, Fe(III) is reduced to Fe(II). (standard potential E^0 ($Fe^{3+} + e^- \leftrightarrow Fe^{2+}$) = 0.77 V) and reacts with $K_3[Fe(CN)_6]$ to form Prussian blue.

This can be measured by CV and spectroscopically by the absorbance of the Prussian blue produced (Figure 14). To do this, light from a halogen lamp was transmitted through the solution via a fiber. The transmitted light was collected by another fiber and fed into a fiber spectrometer. The CV and the change in absorption were detected synchronously. In the backscan from 0.3 V to 1 V the absorbance remains constant. It is clear that the absorption

of the Prussian blue produced becomes broader as the potential scan increases (compare the red, bold spectra in Figure 15) - this is presumably due to the increasing layer on the ITO working electrode.

In the future, a combination of Raman and optical (LED) spectroelectrochemistry will allow synchronous measurements (Figure 16). A suitable notch filter is required to reduce stray light. Figure 15 shows the Raman probe (RP), excitation (EF), read fiber (RF), notch filter (N), SPE and SPE holder (SH).

At least: It was not the intention of this paper to clarify the difference in sensitivity between EC-SERS and absorptovoltammogram measurements, as the electrochemical preparation of colloidal surfaces is sometimes far from being reproducible.

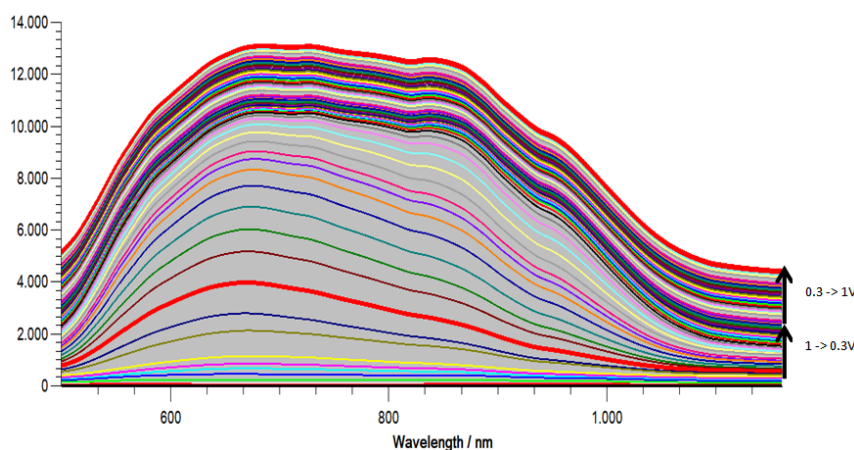


Figure 15. Potential dependent absorption of a solution of $K_3[Fe(CN)_6]$ and Fe(III) salt: Prussian blue was produced at about 0.8 V

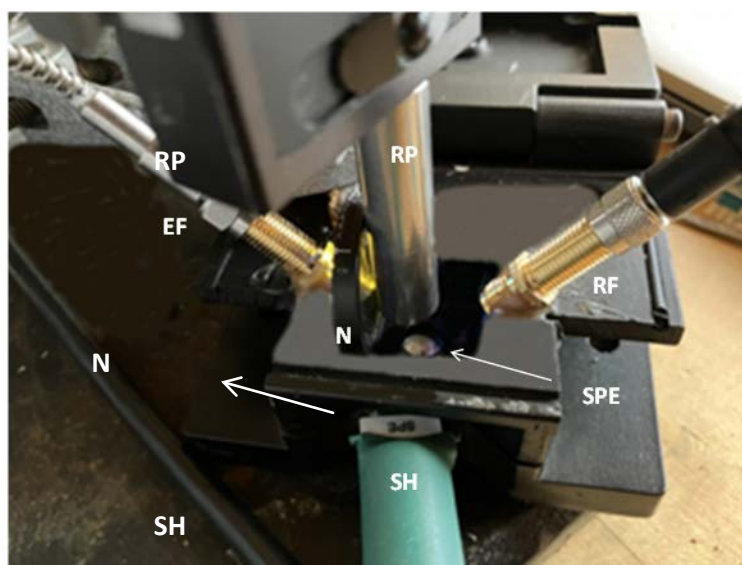


Figure 16. Experimental setup for the synchronous measurement of Raman and LED absorptovoltammetry

3. Conclusion

In conclusion, Raman voltammetry is an instructive method for studying the vibrational changes associated with the redox reaction of the ferri/ferrocyanide couple. To increase the Raman intensity, it is obvious to modify the Au and Ag electrodes used. This can be done by simply potential cycling the electrode covered with a KCl solution. In addition, changes in absorption in the visible spectrum during the ferri/ferrocyanide reaction can be easily measured by combining a cyclic voltammogram with spectroscopic equipment.

The ferri/ferrocyanide system is suitable because the spectroscopic data are known. However, the change in Raman transitions of the ferri/ferrocyanide system on the nanostructured Au and Ag surface shows a strong interaction between adsorbate and adsorbate.

ACKNOWLEDGEMENT

The author would like to thank the Chemical Industry Fund for its support.

References

- [1] M. Fleischmann, P.J. Hendra, A.J. McQuillian, Raman spectra from electrode surfaces, *J. Chem. Soc. Chem Commun.* 1973, 80.
- [2] M. Fleischmann, P.J. Hendra, A.J. McQuillian, Raman Spectra of Pyridine Adsorbed at a Silver Electrode, *Chem Phys. Lett.* 1974, 26,163-166.
- [3] M. Fleischmann, P.R. Graves, J. Robinson, The Raman Spectroscopy of the Ferricyanide/Ferrocyanide System at Gold, b-Palladium Hydride and Platinum Electrodes, *J. Electroanal. Chem.* 1985, 182, 87-98.
- [4] G. Herzberg, *Molecular Spectra and Molecular Structure. II Infrared and Raman Spectra of Polyatomic Molecules*, Van Nostrand Reinhold Company, New York, 1945, p.122.
- [5] B.H. Loo, Y.G. Lee, E.J. Liang, W. Kiefer, Surface-enhanced Raman scattering from ferrocyanide and ferricyanide ions adsorbed on silver and copper colloids, *Chem. Phys. Lett.* 1998, 297, 83-89.
- [6] W.P. Griffith, G.T. Turner, Raman Spectra and Vibrational Assignments of Hexacyano-complexes, *J. Chem. Soc. (A)*, 1970, 858-862.
- [7] D. Ibanez, J. Garoz-Ruiz, A. Heraz, A. Colina, Simultaneous UV-Visible Absorption and Raman Spectroelectrochemistry, *Anal. Chem.* 2016, 88, 8210-8217.
- [8] R. Moldovan, E. Vereshchagina, K. Milenko, B.C. Iacob, A.E. Bodoki, A. Falamas, N. Tosa, C.M. Muntean, C. Farcau, E. Bodoki, Review on combining surface-enhanced Raman

- spectroscopy and electrochemistry for analytical applications, *Anal. Chim. Acta* 2023, 1209, 339250, 1-25.
- [9] D. Martin-Yerga, A. Perez-Junquera, M.B. Gonzalez-Garcia, J.V. Perales-Rondon, A. Heras, A. Colina, D. Hernandez.Santos, P. Fanjul.Bolado, Quantitative Raman spectroelectrochemistry using silver screen-printed electrodes, *Electrochim. Acta*, 2018, 264, 183-190.
- [10] J. Lopez-Palacios, A. Heraz, A. Colina, V. Ruiz, Bidimensional spectroelectrochemical study on electrogeneration of soluble Prussian Blue from hexacyanoferrat (II)solution, *Electrochim. Acta* (2004), 49, 1027-1033.
- [11] L.H. Oakley, D.M. Fabian, H.E. Mayhew, S.A. Svoboda, K.L. Wustholz, Pretreatment Strategies for SERS Analysis of Indigo and Prussian Blue in Aged Painted Surfaces, *Anal. Chem.* (2012), 84, 8006-8012.



© The Author(s) 2024. This article is an open access article distributed under the terms and conditions of the Creative Commons Attribution (CC BY) license (<http://creativecommons.org/licenses/by/4.0/>).